Dalton Transactions

An international journal of inorganic chemistry

Accepted Manuscript

This article can be cited before page numbers have been issued, to do this please use: M. Ksiazek, M. D. Weselski, A. Dreczko, V. Maliuzhenko, M. Kamierczak, A. Tooczko, J. Kusz and R. Bronisz, *Dalton Trans.*, 2020, DOI: 10.1039/D0DT01696A.

ROYAL SOCIETY OF CHEMISTRY

rsc.li/dalton

View Article Online
DOI: 10.1039/D0DT01696A

ARTICLE

Two ways spin crossover in iron(II) coordination polymer associated with conformational changes of bridging ligand

Received 00th January 20xx,
Accepted 00th January 20xx

DOI: 10.1039/x0xx00000x

Maria Książek,[a] Marek Weselski,[b] Agnieszka Dreczko,[b] Vladyslav Maliuzhenko,[b] Marcin Kaźmierczak,[b] Aleksandra Tołoczko,[b] Joachim Kusz,[a] Robert Bronisz [b]*

1,4-di(1-ethyl-1,2,3-triazol-5-yl)butane (**bbtre**) was prepared by lithiation of 1-ethyl-1,2,3-triazole followed then by alkylation with 1,4-dibromobutane. **Bbtre** forms with Fe(II) three-dimensional network $[Fe(\mathbf{bbtre})_3](ClO_4)_2{\cdot}2CH_3CN$ exhibiting thermally induced spin crossover (SCO). Change of temperature or change of spin state results in various types of structural transformations. It leads to formation of different structures which are stable in strictly defined temperature ranges. As a result, there are three spin crossover transitions arranged in two different paths. Thusly, cooling below 280 K involves HT(HS)$\rightarrow$LT(HS) (HT – high temperature structure; LT – low temperature structure) phase transition (PT) which is associated with conformational changes of **bbtre** molecules and with deformation of the polymeric skeleton. In the LT phase there occurs incomplete and reversible LT(HS)$\leftrightarrows$LT(HS/LS) spin crossover. In contrast, rapid cooling (not previously thermally treated sample) allows to avoid HT(HS)$\rightarrow$LT(HS) phase transition and there occurs complete HT(HS)$\rightarrow$HT1(LS) SCO. It means that PT plays a role of switch which allows to choose one of two ways in which SCO will proceed. After rapid cooling, further heating to 150 K and subsequent cooling causes reversible HT1(HS)$\leftrightarrows$HT1(LS) spin crossover ($T_{1/2}^{\downarrow}$= 130 K, $T_{1/2}^{\uparrow}$= 131 K). However raising the temperature to 170-200 K leads to formation of modulated structure HT2(HS) exhibiting next reversible HT2(HS)$\leftrightarrows$HT2(LS) SCO ($T_{1/2}^{\downarrow}$= 121 K, $T_{1/2}^{\uparrow}$ =123 K). Finally heating above 200 K involves HT2(HS)$\rightarrow$LT(HS) PT and resulted LT(HS) structure exhibits incomplete LT(HS)$\leftrightarrows$LT(HS/LS) spin crossover.

Introduction

A search for systems whose spin state can be switched by an external stimuli is one of the greatest challenges of contemporary science.[1,2] Spin crossover, observed in $3d^4$-$3d^7$ octahedral complexes,[3] attracts attention because of a variety of spin state switching methods including: change of temperature, an application of pressure,[4] light irradiation[5] or high frequency pulsing magnetic field.[6] Switching can be also triggered by exploiting ligand-driven light induced spin change,[7] light induced ligand isomerisation[8] as well as chemically by a ligand exchange[9] or as a result of host-guest interactions.[10] Spin state is affected by conformational changes of ligand molecules too.[11,12] Combining predefined functionalities is an important research field[2,13] and spin crossover is a very attractive tool for creating multifunctional materials[14] in which change of spin state involves magnetic ordering,[15] occurrence of SMM[16] (single-molecule magnet) or SCM[17] (single-chain magnet) behavior as well as affects electric conductivity.[18] Spin state also modulates luminescence properties which becomes particularly interesting for systems exhibiting wide hysteresis loop.[19,20]

A key property associated with change of spin state is a variation of metal-ligand distance, particularly large in iron(II) complexes (~0.2Å), which involves reduction of volume of $[FeN_6]$ coordination octahedron at about 25% (~ 3 Å^3).[21] This perturbation can be an origin of further structural changes leading to uncommon properties like: a high stability of light induced high spin form,[22] multiple bistability,[23] multistability,[24] two channel spin crossover.[11] Structural alterations, including conformational flexibility of ligands, may critically affect their properties resulting in reverse spin crossover.[24a,25] Thus, coupling between spin state switching and structural lability is very promising because it creates conditions for an occurrence of complex stimulus-response scenarios.[10c]

The aim of our research is to synthesize spin crossover systems exhibiting structural lability associated with: conformational flexibility of ligands,[26,27] reorientation of coordinated molecules[28] and changes including polymeric layers.[29,30,31,32] In two-dimensional (2D) coordination polymer $[Fe(bbtr)_3](ClO_4)_2$ (bbtr = 1,4-di(1,2,3-triazol-1-yl)butane)[33] change of spin state is accompanied by the structural phase transition related to shift of the neighbouring polymeric layers at about 0.7Å.[29] In contrast to $[Fe(bbtr)_3](ClO_4)_2$, tetrafluoroborate analogue remains in HS form up to 10 K, however, $[Fe(bbtr)_3](BF_4)_2$ exhibits uncommon property which depends on persistent bidirectional switching triggered by laser light irradiation.[34] Also in this case structural phase transition plays

---

[a] *Institute of Physics, University of Silesia, 75 Pułku Piechoty 1, 41-500 Chorzów, Poland.*
[b] *Faculty of Chemistry, University of Wrocław, F. Joliot-Curie 14, 50-383 Wrocław, Poland.*

Electronic Supplementary Information (ESI) available: synthetic procedure of 1-ethyl-1,2,3-triazole, Tables S1-S6, Figures S1-S7. See DOI: 10.1039/x0xx00000x crucial role in displacement of the polymeric layers.[30] Modification of the bbtr ligand which relies on the introduction of a second substituent into 1,2,3-triazole ring allowed preparing 2D networks of $[Fe(ebbtr)_2(CH_3CN)_2]X_2 \cdot 4CH_3CN$ (ebbtr = 1,4-di(5-ethyl-1,2,3-triazol-1-yl)butane, X = ClO_4^-,[31] $CF_3SO_3^-$[27]). In these complexes spin crossover is governed by structural phase transitions too. In perchlorate derivative an occurrence of series of $LS \rightarrow (HS,LS) \rightarrow LS \rightarrow HS$ transitions is accompanied by reorientation of the coordinated/noncoordinated molecules as well as deformation and the mutual shift of the polymeric units. An exchange of perchlorate on triflate anions results in occurrence of ‘normal’’ and ‘’reverse’’ spin crossover which is associated with conformational changes of the bridging ligands. In this complex spin crossover can be accomplished in various ways: as sequence of $HS \leftrightarrows (HS/LS) \leftrightarrows HS \leftrightarrows LS$ transitions as well as in ‘’normal’’ or ‘’reverse’’ mode separately.

An occurrence of uncommon spin crossover properties, associated with presence of the flexible building blocks, was an encouragement to expand studies on another ligands based on skeleton composed from 1,2,3-triazole rings tethered by butylene spacer. Although 1,4-disubstituted-1,2,3-triazoles coordinate monodentately, creating mono- and dinuclear iron(II) spin crossover complexes,[35] they can also act as μ-κ^2*N2*,*N3* bridging molecules. Therefore, taking into account exclusively monodentate coordination fashion of 1,5-disubstituted-1,2,3-triazoles, we have focused on synthesis of novel ligands in which 1,5-disubstituted rings are, in contrast, joined through carbon atoms. An application of 1,4-di(1-ethyl-1,2,3-triazol-5-yl)butane (**bbtre**) resulted in structurally labile 3D network $[Fe(\mathbf{bbtre})_3](ClO_4)_2 \cdot 2CH_3CN$ (**1**) in which complex spin crossover is governed by conformational changes of **bbtre** molecules. However, **1** exhibits completely different properties in comparison with ebbtr based systems because, instead of reverse spin crossover, there occurs three spin crossover arranged in two paths.

Results and discussion

1,4-di(1-ethyl-1,2,3-triazol-5-yl)butane was prepared by lithiation of 1-ethyl-1,2,3-triazole followed then by alkylation with 1,4-dibromobutane. The ligand was isolated with 34% yield as colorless crystalline solid, soluble in common solvents like: acetonitrile, methanol or dichloromethane. The crystal structure determined for **bbtre** confirmed localization of the 1,4-butylene spacer on C5 carbon atoms of the triazole rings (Fig. 1, Table S1).

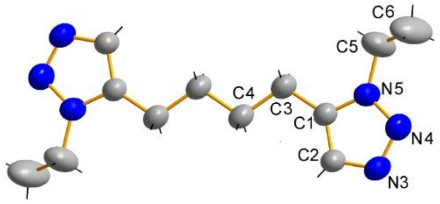

Figure 1. Molecular structure of **bbtre** (CH bonds are marked by thin lines).

View Article Online
DOI: 10.1039/D0DT01696A

Reactions between **bbtre** and iron(II) perchlorate hexahydrate, performed in acetonitrile, results in colorless crystals of $[Fe(\mathbf{bbtre})_3](ClO_4)_2 \cdot 2CH_3CN$ (**1**). Crystalline samples of **1** are unstable outside the mother liquor and therefore magnetic and Mössbauer spectroscopy studies were carried out for samples moistened with acetonitrile.

The complex crystallizes in triclinic crystal system (P-1, Table S2) denoted as HT(HS)). At 295 K there is one crystallographically independent iron(II) ion in the crystal lattice. **1** represents unique example of the complex based on 1,5-disubstituted-1,2,3-triazole type ligands in which the first coordination sphere is composed exclusively from six azole rings (Fig. 2). In comparison with mono 1-substituted 1,2,3-triazoles, which form homo- and heteroleptic complexes, among all known examples based on 1,5-disubstituted-1,2,3-triazoles, only heteroleptic systems were isolated to date. In **1** ligand molecules are connected with iron(II) through *exo* positioned nitrogen atoms N3.

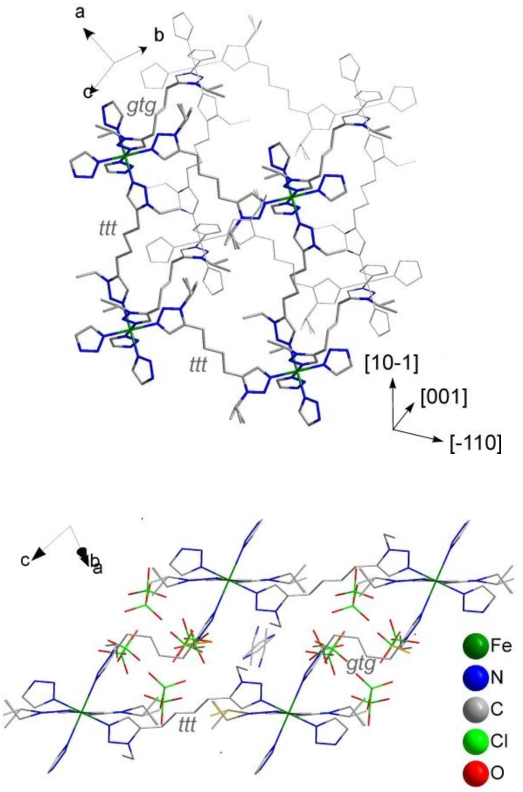

a)

b)

Figure 2. Fragment of the three-dimensional network together with coordination environment of iron(II) in **1** at 295 K (HT(HS) structure) showing two neighboring layers (colored, thick lines and grey, thin lines) which are crosslinked by **bbtre** molecules adopting *gtg* conformation (colored, thick lines) (a) and arrangement of anions and acetonitrile molecules between layers (b). Hydrogen atoms are omitted for clarity. Motif of single layer (marked by thick lines) was exploited on Figure 4 to present conformational changes which occurs only within the layer.

The Fe1-N(triazole) bond lengths are equal to 2.162(5), 2.167(5) and 2.201(5) Å and are characteristic for high spin form of the complex (Table S3). The range of the N-Fe-N angles is from 88.8(2) to 92.1(2)°. Thus, the geometry of the

View Article Online
DOI: 10.1039/D0DT01696A

coordination octahedron is very similar to the one found in the family of $[Fe(bbtr)_3]X_2$ ($X=ClO_4^-$, BF_4^-) complexes as well as in the complexes based on 1-substituted tetrazoles.[36] Inspection of torsion angles indicates that **bbtre** molecules adopt two types of conformations: *trans-trans-trans* (*ttt*) and *gauche-trans-gauche* (*gtg*). Molecules adopting *ttt* conformation link iron(II) ions arranged in [-110] and [10-1] directions which results in two-dimensional polymeric layer (Fig. 2a). Iron(II) ions from neighbouring layers are linked in [001] direction by ligand molecules adopting *gtg* conformation which leads to formation of the three-dimensional (3D) network of α-Po topology (Fig. 2b, Fig. S1). Iron(II) ions linked in [-110], [10-1], and [001] directions are separated at distances 13.7, 13.8 and 12.6 Å, respectively. Ethyl substituents of ligand molecules, bridging metal ions in [-110] and [001] directions, are disordered. Perchlorates form intermolecular contacts with disordered butylene chains and with triazole rings. Noncoordinated acetonitrile molecules are disordered, too.

The path from HT(HS) to LT(LS).

Results of magnetic studies show that in the temperature range 150-300 K the complex **1** remains in the HS form. Lowering of temperature below 150 K ($\chi_M T$ = 3.45 cm^{3}Kmol^{-1}) involves gradual reduction of $\chi_M T$ indicating change of the spin state of iron(II) ions (Fig. 3a). Spin crossover is finished at 70 K however it is incomplete and about 70% of iron(II) ions still remains in HS form ($\chi_M T$ = 2.5 cm^{3}Kmol^{-1}). In the heating mode the $\chi_M T(T)$ dependence is practically the same as during cooling.

Mössbauer spectrum of **1** recorded at 260 K indicates presence of one doublet with isomer shift and quadrupole splitting parameters of values δ = 1.16 mm/s and ΔE_Q= 1.70 mm/s, respectively, characteristic for HS form of the octahedral iron(II) complex. Below 160 K a single line with δ = 0.55 mm/s corresponding to low spin form of the complex appears (Fig. 3a inset). At 70 K the relative area of HS component $A_{HS}/(A_{HS} + A_{LS})$ (A_{HS} – peak area of HS doublet, A_{LS} – peak area of LS singlet) equals to 0.72 which remains in agreement with results of magnetic studies. During heating the temperature dependence of relative area of HS form is practically the same as it was found during cooling (Fig. 3a).

Multitemperature single crystal X-ray diffraction studies revealed occurrence of the crystallographic phase transition below 280 K. At 200 K the Fe-N distances are in the range from 2.192(4) to 2.207(4) Å, thus they are characteristic for HS form (Table S4). Formation of LT(HS) structure is accompanied by the change of the ligand conformation. The changes occurs exclusively within the layers (Fig. 4, Fig. S2). In LT(HS) structure (Fig. 4b), in bridging direction corresponding to [-110] in HT(HS) structure, a half of **bbtre** molecules change the conformation from *ttt* to *gtg.* It results in significant shortening of distance between bridged iron(II) ions from 13.8 to 12.6 Å. In the second bridging direction (corresponding to [10-1] in HT(HS) structure) every second molecule changes its conformation from *ttt* to *gtg* with simultaneous disordering over two positions (occupancy factor = 0.5). Also in this case reduction of the distance between bridged iron(II) ions from 13.8 to 12.6 Å takes place. In comparison, separations between iron(II) ions still bridged by *ttt* conformers is only slightly reduced of about 0.05 Å.

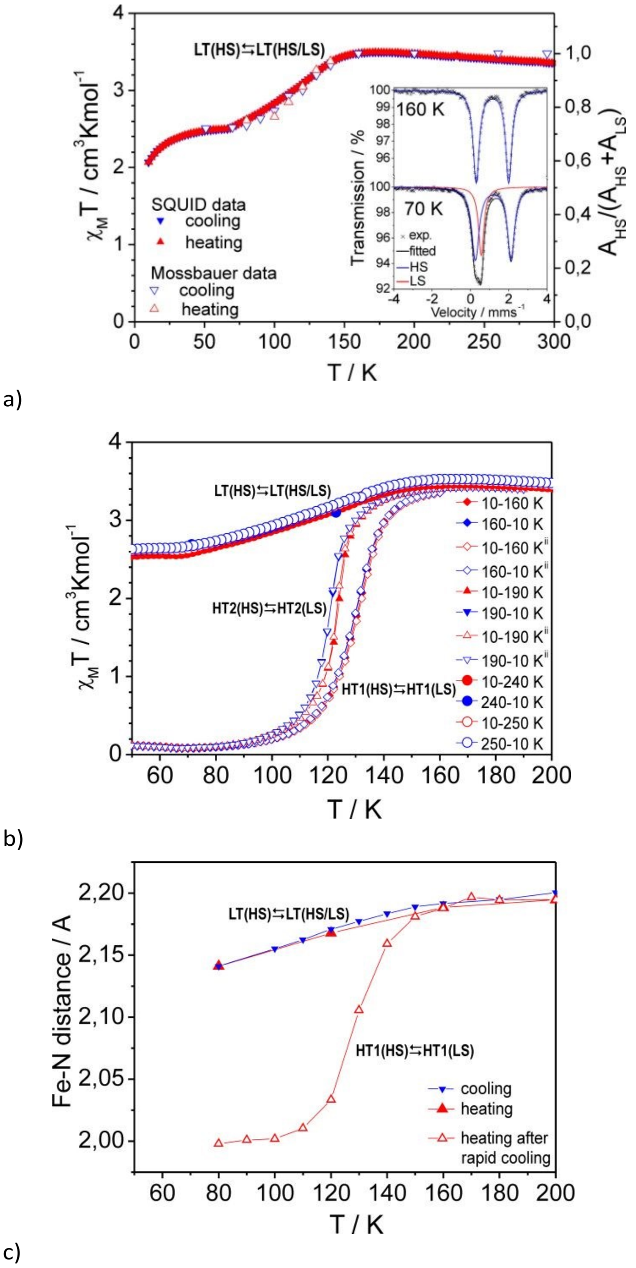

Figure 3. Temperature dependences of $\chi_M T$ (1K/min, filled triangles) together with relative areas of HS form component ($A_{HS}/(A_{HS}+A_{LS})$) derived from Mössbauer spectra (open triangles) recorded in cooling and heating mode (a), series of selected $\chi_M T(T)$ dependences (heating/cooling cycles) recorded after initial rapid cooling of sample at 10 K (b), average Fe-N distances determined during cooling/heating (first crystal, filled triangles) as well as in the heating mode after rapid cooling (second, previously not thermally treated crystal, open triangles) (c). Cooling mode is marked by blue and heating by red colour (figures a, b and c).^{ii} - denotes second heating/cooling cycle carried out in the same temperature range as previous one. Magnetic and Mössbauer spectroscopy studies were carried out for samples (the same synthetic batch) moistened with acetonitrile.

View Article Online
DOI: 10.1039/D0DT01696A

Nonequivalence of iron···iron separations causes the polymeric grid to deform (Fig. 5a) and resulted strains entail corrugation of the layer - iron atoms deviate from least-squares plane at about 0.7-0.8 Å (Fig. 5b, Fig. S2). Ligands adopting *gtg* conformation in HT(HS) remain unchanged in LT(HS) structure and distance between bridged iron(II) ions still equals 12.6 Å.

Further cooling leads to gradual and incomplete LT(HS)→LT(HS/LS) spin crossover (Fig. 3c). At 80 K Fe-N distances are in the range 2.130(5) - 2.148(5) Å. Taking into account shortening of Fe-N distance at *ca.* 0.2 Å, expectable for complete spin crossover, it can be estimated that about 70% iron(II) ions remain in HS form. Distances between bridged iron(II) ions in LT(HS/LS) structure are shorter at 0.1 Å in comparison with LT(HS) structure. Spin crossover does not involve significant structural changes of bridging ligands (Fig. 4c, Table S4) and polymeric layers remain corrugated.

Heating of the crystal from 80 to 280 K does not lead to restoration of initial HT(HS) structure and the complex exists in LT(HS) structure. It is worth adding that cooling (not previously thermally treated crystal) from 300 to 240 K, that is below temperature of structural phase transition, followed then by its heating again to 280 K, does not allow to restore HT(HS) structure, too. Hence, structural phase transition is not reversible in the investigated temperature range.

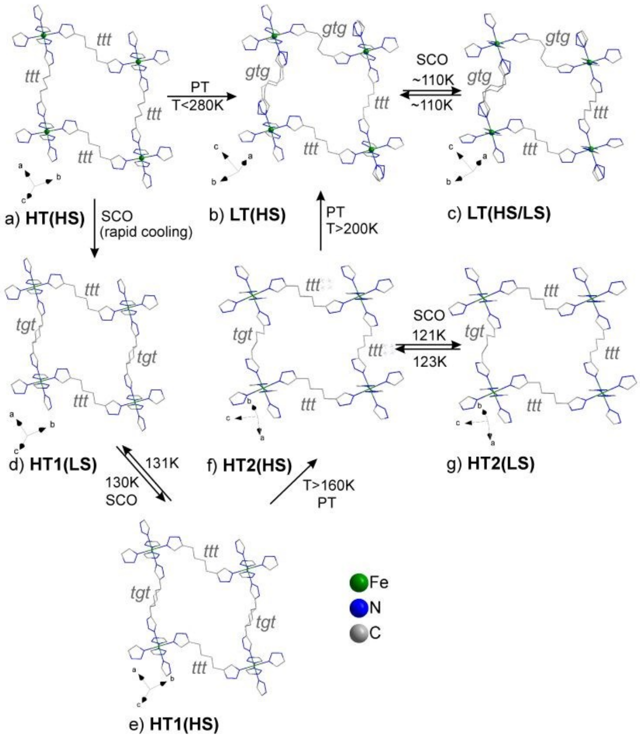

Figure 4. Scheme showing occurred phase transitions (PT) and spin crossover (SCO) in **1** together with conformations (*t = trans, g = gauche*) of **bbtre** molecules (ethyl substituents were removed for clarity) in: HT(HS) structure at 295 K (a), LT(HS) at 200K (b), LT(HS/LS) at 80K (c), HT1(LS) at 80K, (d) HT1(HS) at 150 K (e), HT2(HS) at 170 K (f), HT2(LS) at 80 K (g). $T_{1/2}$ values for reversible SCO are placed together with suitable arrows.

The path from HT(HS) to HT1(LS).

Recent studies of the complexes based on 1,4-di(5-ethyl-1,2,3-triazol-1-yl)butane[27,31] and tris(n-butyl-imidazol(2-ethylamino))amine[11,37] revealed that phase transitions, in particular associated with structural changes of ligands, may play a role of steering switch to various phases which exhibit different spin crossover properties. Therefore, in order to test such possibility, we have tried to suppress occurrence of HT(HS)→LT(HS/HS) transition by rapid cooling (sample was placed in the chamber of SQUID magnetometer cooled to 10 K). It is well known that usually fast cooling can lead to partial or complete quenching of the HS→LS transition.[38] In contrast, rapid cooling of **1** at 10 K results surprisingly in complete switching to low spin form (denoted further as HT1(LS)). Moreover, subsequent measurement performed in the heating mode revealed an occurrence of abrupt HT1(LS)⇆HT1(HS) spin crossover (Fig. 3b).

X-ray diffraction studies on single crystals placed directly into the stream of nitrogen at 80 K were carried out to understand structural processes related to rapid cooling. In contrast to gradual and incomplete LT(HS)⇆LT(HS/LS) spin crossover, rapid cooling is accompanied by significant shortening of Fe-N distances to 2.002(2), 2.002(2) and 2.011(2) Å (Table S5). It results in formation of new HT1(LS) phase, which means suppression of HT(HS)→LT(HS) transition. In HT1(LS) structure **bbtre** molecules, linking iron(II) ions in [10-1] direction change their conformation from *ttt* to *tgt* (*trans-gauche-trans*) (Fig. 4d) and become disordered in two positions (o.f. = 0.5). Conformation of ligand molecules linking iron(II) ions in [-110] and [001] directions remain unchanged. Formation of HT1(LS) structure is accompanied by shortening of iron···iron distances in all bridging directions at 0.2-0.3 Å. In comparison to HT(HS)→LT(HS) transition, rapid cooling does not involve deformation of the polymeric layers. Noncoordinated acetonitrile molecules as well as perchlorate anions are disordered.

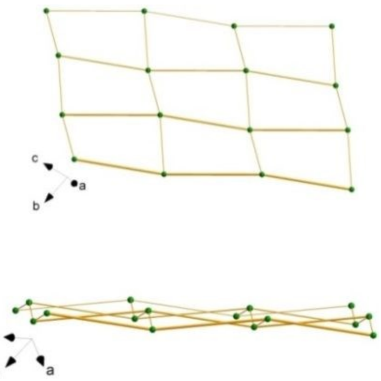

Figure 5. Schematic presentation of LT(HS) structure showing deformation of the layer grid (a) and corrugation of the polymeric layer (b) as a result of HT(HS)→LT(HS) structural phase transition in **1**. Orange lines mark ligand molecules linking iron(II) ions (green balls).

An elevation of temperature to 150 K is accompanied by increasing the Fe-N distances to values characteristic for HS form of the complex (Table S5). Formation of HT1(HS) structure (Fig. 4e) is reversible and cooling to 80 K leads to HT1(LS) structure (Fig. 4d).

It was found that heating of the crystal to temperature 170-200 K is accompanied by appearance of very weak satellite reflections with a modulation vector **q**=(0.303, 0.300, 0.406) leading to *ca.* seven times enlarged volume of the unit cell for the superstructure (at 80K unit cell parameters for the average structure are a=10.4994(2)Å, b=12.2450(4)Å, c=12.1324(3)Å, α=84.628(2)°, β=73.4236(19)°, γ=72.557(2)°, V=1426.18(6)$Å^3$, while for the superstucture are a=13.5837(5)Å, b=24.1794(8)Å, c=31.1525(11)Å, α=77.484(3)°, β=88.255(3)°, γ=87.785(3)°, V=9978.7(6)$Å^3$). The characteristic feature of novel HT2(HS) structure (Fig. 4f) is long range ordering of ligand molecules. In the modulated structure **bbtre** molecules adopt alternately *tgt* and *ttt* conformations in the bridging direction corresponding to [10-1] in HT(HS) structure. In HT2(HS) structure iron(II) ions occupy common plane and corrugation of the polymeric layer is not observed. However, we have determined only the tentative model of the modulated HT2(HS) structure because satellite reflections are very weak. In the average structure (Table S6, Fig. S2) a presence of two **bbtre** conformers is visible as a ligand disorder occurring in [10-1] direction. It should be noticed that similar behavior depending on a long range ordering of ligand molecules, triggered by the change of temperature or spin crossover, occurs in another three-dimensional coordination polymer $[Fe(qbtr)_3](ClO_4)_2$ (qbtr=1,5-di(1,2,3-triazol-1-yl)pentane).[26b] It is worth to add that in 1D systems based on ligands possesing expanded spacer like 1,3-bis((1H-tetrazol-1-yl)methyl)bicyclo[1.1.1]pentane or *m*-xylylenebis(tetrazole) ligand disorder is not observed.[39] After lowering of temperature from 170 to 80 K satellite reflections in **1** are still present indicating the existence of a long range ordering of **bbtre** molecules (Fig. 4g).

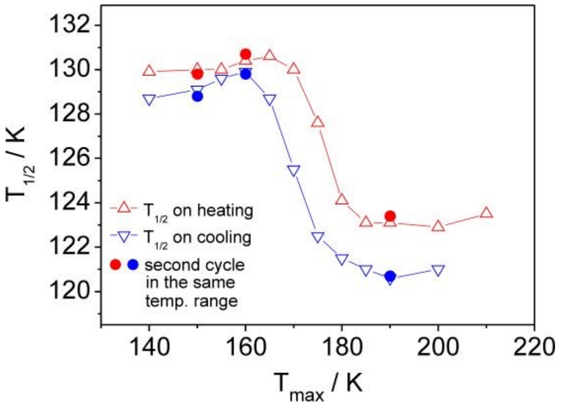

Figure 6. Dependence of $T_{1/2}{\downarrow}$ (blue) and $T_{1/2}{\uparrow}$ (red) versus highest temperature T_{max} reached during heating. Filled symbols denote $T_{1/2}{\downarrow}$ and $T_{1/2}{\uparrow}$ values obtained as a result of second heating/cooling cycle carried out in the same temperature range immediately after reaching T_{max} value for the first one. The points on the plot were determined on the basis of the measurements which are shown on Figure S4 (it contains full experimental protocol).

Thus, HT2(HS)→HT2(LS) is not associated with conformational changes of bridging ligands. Inspection of the Fe-N distances in the average structure shows complete spin crossover (Table S6). Re-heating to 170-200 K again results in modulated HT2(HS) structure which confirms reversibility of HT2(HS)⇆HT2(LS) spin crossover.

It is worth noticing that cell volumes (calculated for one molecule of the complex) decreases for LT(HS/LS) (1457.9 $Å^3$), HT1(LS) (1452.5 $Å^3$) and HT2(LS) (1426.2 $Å^3$) structures determined at 80 K. It corresponds to increase of abruptness of SCO and can indicate an importance of crystal packing effects.

An occurrence of HT1(HS)→HT2(HS) structural phase transition has been confirmed by magnetic studies carried out on a sample rapidly frozen at 10 K. Raising the temperature, in steps by 5 or 10 K on each consecutive heating/cooling cycle, revealed two sets of spin crossover dependences (Fig. 3b, Fig. S3). Heating to 160 K results in abrupt and complete spin crossover with $T_{1/2}{\uparrow}\cong 131$ K and $T_{1/2}{\downarrow}\cong 130$ K. Further elevation of the heating limit to 180 K involves abrupt lowering of SCO temperatures to values of $T_{1/2}{\uparrow}\cong 123$ K and $T_{1/2}{\downarrow}\cong 121$ K.

A dependence of $T_{1/2}$ *vs.* maximum heating temperature T_{max} (Fig. 6) shows a discontinuity (165-175 K) which corresponds to results of diffraction studies and indicates that HT1 and HT2 structures have different spin crossover properties. It is worth noticing that differential scanning calorimetry (DSC) measurements revealed, in accordance with results of magnetic studies, shift of peaks to lower temperatures after reaching 180 K (Fig. S4).

Finally, raising the temperature above 200 K results in conformational changes of **bbtre** molecules leading to reconstruction of LT(HS) structure (Fig. 4b). It explains why after rapid cooling, followed then by heating to 300 K, only gradual and incomplete spin crossover occurs during next cooling/heating cycles. Experiments depending on annealing sample at 330 K followed then by rapid cooling to 10 K did not allow to obtain abrupt and complete spin crossover, thus formation of LT(HS) structure is irreversible.

What is important the uncommon behavior, presented here, is not associated with the change of the chemical composition.[40]

Summary

In this report we have presented synthesis of 1,4-di(1-ethyl-1,2,3-triazol-5-yl)butane (**bbtre**) and its application to preparation of iron(II) spin crossover systems. A presence of 1,4-butylene spacer together with additional alkyl substituent was dictated by need to increase ligands flexibility, thus, facilitating occurrence of structural lability of the complexes. This approach has been successfully realized in the case of three-dimensional coordination polymer $[Fe(\textbf{bbtre})_3](ClO_4)_2{\cdot}2CH_3CN$ prepared in the reaction of bbtre with iron(II) perchlorate. In this complex, conformational changes *ttt*→*gtg* (*t* = *trans*, *g* = *gauche*), associated with HT(HS)→LT(HS) structural phase transition upon cooling below 280 K, play a role of the switch which allows to perform spin crossover in two ways. Thus, further cooling involves below 150 K reversible, gradual and incomplete LT(HS)$\leftrightarrows$LT(HS/LS) spin crossover. In contrast, rapid cooling triggers complete HT(HS)$\rightarrow$HT1(LS) spin crossover which is accompanied by *ttt*$\rightarrow$*tgt* transformations of **bbtre** molecules. In the heating mode spin crossover behaviour is complex in nature. Raising of temperature to 150-160 K triggers abrupt and reversible HT1(LS)$\leftrightarrows$HT1(HS) spin crossover with $T_{1/2}{}^{\downarrow}$= 130 K and $T_{1/2}{}^{\uparrow}$ =131 K. An elevation of temperature to 170-200 K is associated with formation of modulated HT2(HS) structure. Also in this case it is possible to carry out reversible and complete spin crossover HT2(HS)$\leftrightarrows$LT2(LS) ($T_{1/2}{}^{\downarrow}$= 121 K and $T_{1/2}{}^{\uparrow}$ =123 K). Modulation of the crystal structure HT2 in the low spin form of the complex is preserved and hence a return to HT1 structure is not possible. Finally, heating above 200 K leads to reconstruction of LT(HS) structure, thus, gradual and incomplete LT(HS)$\leftrightarrows$LT(HS/LS) spin crossover in the next cooling/heating cycles can be realized. HT(HS)$\rightarrow$LT(HS) and HT2(HS)$\rightarrow$LT(HS) transitions are irreversible, therefore, accomplishment of LT(HS) phase does not allow to repeat (after next rapid cooling) abrupt and complete spin crossover and LT(HS)$\leftrightarrows$LT(HS/LS) spin crossover can be carried out.

Results, presented in this paper, show importance of implementation of potentially structurally labile building blocks as functionalities increasing an inclination to occur structural phase transitions governing properties of the material. It is clearly visible that assembling in one material of spin crossover and conformational flexibility remarkably increases complexity of stimulus-response but, what is important, allowing behave control over the state of the system. It support recent studies on spin crossover systems based on 1,4-di(5-ethyl-1,2,3-triazol-1-yl)butane[27,31] and tris(n-butyl-imidazol(2-ethylamino))amine[11] in which structural phase transitions allow to switch properties by choice of desired spin crossover active phase.

Experimental

Materials and methods. HPLC grade THF (Across) was dried for two weeks over molecular sieves 3A activated at 160°C.[41] 1,4-dibromobutane purchased from Aldrich was distilled and stored also over molecular sieves 3A. Dichloromethane (POCh) was distilled prior to use. Hexane solution of *n*-BuLi (2.5M, Aldrich), acetonitrile (HPLC grade, Across), sodium sulfate anhydrous, silica gel (Merck, K60, 230-400 mesh) and iron(II) perchlorate hexahydrate were used as delivered without further purification. Acetonitrile used to synthesis of the complexes was distilled over the calcium hydride.

Elemental analyses for carbon, hydrogen and nitrogen were performed on Perkin Elmer 240C analyzer. ^{1}H NMR and ^{13}C NMR spectra were recorded on AMX Bruker NMR 500 MHz spectrometer at room temperature in $CDCl_3$ solutions. IR spectra of **bbtre** (KBr pellet) and 1 (nujol mull) were recorded with the Jasco FT/IR-4700 spectrometer in the range 400-4000 cm^{-1}. Temperature dependent measurements of the magnetic susceptibility of complexes were carried out with a Quantum Design SQUID magnetometer under 1T applied magnetic field. Measurements were carried out with rate 1 K/min (cooling, heating). The only exception is generation of HT1(HS) phase depending on rapid cooling below phase transition. All magnetic measurements were carried out for samples moistened with acetonitrile and placed in the sealed glass tube. Magnetic data were corrected for signal of glass tube and for the diamagnetic contributions of the sample, which were estimated from Pascal's constants. DSC measurements (Fig. S4) were carried out with Mettler Toledo DSC 3 at 2 K min^{-1}. Mössbauer spectra were recorded using ^{57}Co/Rh source (*ca.* 10mCi) on POLON spectrometer working at constant acceleration mode. The sample (ca. 100 mg) moistened with acetonitrile was placed in the sealed plastic container and mounted on a cold finger of helium cryostat (ARS DMX-20 cooling system). The isomer shift δ and quadrupole splitting ΔE_Q were calculated in relation to α-Fe (295 K).

Caution! Even though no problems were encountered it is worth to mention that complexes containing perchlorates are potentially explosive and should be synthesized in milligram scale and handled with care.

X-ray data collection and structure determination. The crystals of complexes suitable for X-ray measurements were obtained directly from syntheses of macroscopic samples and preselected using the stereoscopic Zeiss microscope under nitrogen atmosphere. For the X-ray measurements single crystals of the complexes were placed on the loops in the drop of oil. The measurement of single crystal of bbtre was performed with a four-circle Xcalibur X-ray diffractometer equipped with Sapphire3 CCD detector and Mo-Kα (λ = 0.71073 Å) radiation. The controlling of the measurement procedure and data reduction were performed by CrysAlis^{Pro} software.[42] Structural studies of complex 1 were performed with a four-circle SuperNova X-ray diffractometer with microfocus X-ray tube, optimized multi-layer optics for Mo-Kα (λ = 0.71073 Å) or Cu-Kα (λ = 1.54184 Å) radiation and an Atlas CCD detector. In these cases the controlling of the measurement procedure and data reduction were performed also by CrysAlis^{Pro} software.[43] The same program was used to determine and refine the lattice parameters. Low temperatures were achieved with a stream of cold nitrogen gas (Oxford Cryosystem cooling device); the temperature stability was 0.1 K.

The structures were solved by direct methods and subsequently completed by the difference Fourier. All the non-hydrogen atoms were refined using full-matrix, least-squares technique. The hydrogen atoms were treated as riding on their parent carbon atoms with isotropic displacement parameters (equal 1.2 or 1.5 times the value of C displacement parameters). The structures were severely disordered, therefore various constraints and restraints were used during refinement (EADP, EXYZ, DFIX, DANG, SAME). SHELXS-2013

View Article Online
DOI: 10.1039/D0DT01696A

and SHELXL-2018/3 programs were used for the calculations.[44] CCDC 1885384 (compound **bbtre**) and 1953184 - 1953190 (compound **1**) contain the supplementary crystallographic data for this paper. These data can be obtained free of charge from The Cambridge Crystallographic Data Centre via www.ccdc.cam.ac.uk/data_request/cif

Synthesis of 1-ethyl-1,2,3-triazole.[45] In 1000 mL round bottom flask 1,2,3-triazole (69.06 g, 1.0 mol) and water (50 mL) was placed and then solution of NaOH (39.99 g, 1.0 mol) in water (150 mL) was added in few portions. Water was removed under reduced pressure using rotary evaporator. The white solid was dried by aseotropic distillation with acetonitrile. CH_2Cl_2 (400 mL) was added to resulted product. Then diethyl sulfate (128.5 mL, 1.0 mol) was dropped over the time 80 minutes to ice cooled mixture. Reaction mixture was stirred at room temperature for seven days and then the white solid was filtered off and solvent was removed under reduced pressure. 2-ethyl-1,2,3-triazole (2etr) was isolated by fractional distillation under atmospheric pressure collecting fraction boiling at temperature range 113-115°C. 1-ethyl-1,2,3-triazole (1etr) was isolated by distillation under reduced pressure (8 mmHg). The fraction boiled at 86-87°C was collected. Yield 36.8g (38%) for 1etr. ^{1}HNMR ($CDCl_3$) δ: 7.68 (s, 1H, *H*-tr), 7.54 (s, 1H, *H*-tr), 4.43 (q, 2H, ^3J=7.5 Hz, tr-C*H*$_2$-CH$_3$), 1.54 (t, 3H, ^3J=7.4 Hz, tr-CH$_2$-C*H*$_3$) ppm. ^{13}CNMR ($CDCl_3$) δ: 133.9, 122.7, 45.2, 15.6 ppm. See Fig. S5a for FTIR spectrum. Yield 17.1g (18%) for 2etr. ^{1}HNMR ($CDCl_3$) δ: 7.56 (s, 2H, *H*-tr), 4.47 (q, 2H, ^3J=7.3 Hz, tr-C*H*$_2$-CH$_3$), 1.54 (t, 3H, ^3J=7.3 Hz, tr-CH$_2$-C*H*$_3$) ppm. ^{13}CNMR ($CDCl_3$) δ: 134.0, 50.0, 14.9 ppm. See Fig. S5b for FTIR spectrum.

Synthesis of 1,4-di(1-methyl-1,2,3-triazol-5-yl)butane (bbtre). Glassware was dried before use at 130°C in an oven and cooled under stream of nitrogen. Synthesis was carried out in the nitrogen atmosphere. Dry THF (260 mL) was placed In three-necked flask (equipped with thermometer, oil bubbler and septum), cooled to -40°C (dry ice/isopropanol/ethanol bath) and then *n*-BuLi (17.7 mL, 44.2 mmol) was added. Then 1-ethyl-1,2,3-triazole 4.09 g (42.1 mmol) in THF (10 mL) was added in a few portions followed by addition of dibromobutane (4.32 g, 20.0 mmol). The reaction mixture was stirred for 2h. Then the flask was removed from cooling bath and allowed to reach room temperature within 2h. Water (15 mL) was poured into reaction mixture. Solvents were distilled under reduced pressure using rotary evaporator. Obtained solid matter was dissolved in water (15 mL) and extracted with hexane (2x20 mL) and then with dichloromethane (5x50 mL). Dichloromethane fractions were collected and dried over anhydrous sodium sulphate. Dichloromethane was distilled off and crude product was recrystallized from isopropanol. Yield 1.29 g (26.0%) colourless crystals. Anal. found: C, 57.9; H, 8.5; N, 33.7 %. Calc. for $C_{12}H_{20}N_6$ (M_w=248.33 g/mol): C, 58.0; H, 8.1; N, 33.8 %. ^{1}HNMR ($CDCl_3$) δ: 7.42 (s, 2H, *H*-tr), 4.27 (q, 4H, ^{3}J = 7.45 Hz, tr-C*H*$_2$-CH$_3$), 2.68 (m, 4H, tr-C*H*$_2$-CH$_2$-), 1.78 (m, 4H, tr-CH$_2$-C*H*$_2$-) 1.49 (t, 6H, ^{3}J = 7.45 Hz, tr-CH$_2$-C*H*$_3$) ppm; ^{13}CNMR ($CDCl_3$) δ: 135.82, 132.14, 42.84, 27.87, 23.02, 15.52 ppm. See Fig. S6 for IR spectrum.

Synthesis of [Fe(bbtre)$_3$](ClO$_4$)$_2$·2CH$_3$CN (1). Syntheses of the complex were carried out under nitrogen atmosphere using the standard Schlenk technique. To the solution of **bbtre** (0.20 mmol, 49.6 mg). in acetonitrile (5 mL) the solution of $Fe(ClO_4)_2{\cdot}6H_2O$ (0.10 mmol, 36.3 mg) in acetonitrile (5mL) was added. The obtained colorless solution was left in the closed Schlenk flask. After 2 days, colorless crystals were filtered off. Yield 29.0 mg. Anal. found: C, 44.2; H, 6.2; N, 26.2%. Calc. for $FeC_{40}H_{66}N_{20}Cl_2O_8$ (M_w=1081.83): C, 44.4; H, 6.1; N, 25.9 %. See Fig. S7 for IR spectrum.

Conflicts of interest

There are no conflicts to declare.

Acknowledgements

This work was supported by the Polish National Sciences Centre Grant No. DEC-2014/15/B/ST5/04771. We are grateful to Professor T. Lis for the consultation and valuable remarks.

References

1 O. Sato, *Nat. Chem*. 2016, **8**, 644.
2 a) K. S.Kumar and M. Ruben, *Coord. Chem. Rev*. **2017**, *346*, 176-205; b) S. Kitagawa and R. Kitaura, S. Noro, *Angew. Chem. Int. Ed.* 2004, **43**, 2334.
3 a) P. Gütlich, A. Hauser and H. Spiering, *Angew. Chem., Int. Ed. Engl*., 1994, **33**, 2024; b) P. Gütlich, Y. Garcia and H. A. Goodwin, *Chem. Soc. Rev*., 2000, **29**, 419; c) M. C. Munoz and J. A. Real, *Coord. Chem. Rev*., 2011, **255**, 2068; d) M. A. Halcrow, *Chem. Soc. Rev*., 2011, **40**, 4119-4142.
4 V. Ksenofontov, A. B. Gaspar and P. Gütlich, *Top. Curr. Chem*. 2004, **235**, 23.
5 S. Decurtins, P. Gutlich, C. P. Kohler, H. Spiering and A. Hauser, *Chem. Phys. Lett*. 1984, **105,** 1-4.
6 A. Bousseksou, F. Varret, M. Goiran, K. Boukheddaden and J. P. Tuchagues, *Top. Curr. Chem*. 2004, **235**, 65.
7 M.-L. Boillot, J. Zarembowitch and A. Sour, *Top. Curr. Chem*. 2004, **234**, 261.
8 a) B. Rosner, M. Milek, A. Witt, B. Gobaut, P. Torelli, R. H. Fink and M. M. Khusniyarov, *Angew. Chem. Int. Ed.* 2015, **54**, 12976; b) Y. Hasegawa, K. Takahashi, S. Kume and H. Nishihara, *Chem. Commun*. 2011, **47**, 6846.
9 a) V. Niel, A. L. Thompson, M. C. Munoz, A. Galet, A. E. Goeta and J. A. Real, *Angew. Chem. Int. Ed*. 2003, **42**, 3760; b) A. Galet, M. C. Munoz and J. A. Real, *Chem. Commun*. 2006, 4321.
10 a) M. Ohba, K. Yoneda, G. Agusti, M. C. Munoz, A. B. Gaspar, J. A. Real, M. Yamasaki, H. Ando, Y. Nakao, S. Sakaki and S. Kitagawa, *Angew. Chem., Int. Ed*. 2009, **48**, 4767; b) R. Ohtani, S. Hayami, *Chem. Eur. J*. 2017, **23**, 2236.
11 M. Seredyuk, M. C. Munoz, M. Castro, T. Romero-Morcillo, A. B. Gaspar and J. A. Real, *Chem. Eur. J*. 2013, **19**, 6591.
12 a) T. Fujinami, K. Nishi, D. Hamada, K. Murakami, N. Matsumoto, S. Iijima, M. Kojima and Y. Sunatsuki, *Inorg. Chem*. 2015, **54**, 7291; b) G. S. Matouzenko, A. Bousseksou,

S. A. Borshch, M. Perrin, S. Zein, L. Salmon, G. Molnar and S. Lecocq, *Inorg. Chem*. 2004, **43**, 227.

13 C. Janiak, *J. Chem. Soc. Dalton Trans*. 2003, 2781.

14 a) A. Halcrow, Spin-Crossover Materials: Properties and Applications. Wiley-VCH, Weinheim, 2013; b) G. Molnár, S. Rat, L. Salmon, W. Nicolazzi and A. Bousseksou, *Adv. Mater*. 2018, **30**, 17003862; c) A. Bousseksou, G. Molnar, L. Salmon and W. Nicolazzi, *Chem. Soc. Rev*., 2011, **40**, 3313.

15 a) S. I. Ohkoshi, K. Imoto, Y. Tsunobuchi, S. Takano and H. Tokoro, *Nature Chem*. 2011, **3**, 564; b) D. Pinkowicz, M. Rams, M. Mišek, K. V. Kamenev, H. Tomkowiak and A. Katrusiak, B. Sieklucka, *J. Am. Chem. Soc*., 2015, **137**, 8795.

16 a) X. Feng, C. Mathonière, J. Ie-R, Jeon, M. Rouzières, A. Ozarowski, M. L. Aubrey, M. I. Gonzalez, R. Clérac and J. R. Long, *J. Am. Chem. Soc.* 2013, **135**, 15880; b) C. Mathonière, H.-J. Lin, D. Siretanu, R. Clérac and J. M. Smith, *J. Am. Chem. Soc*. 2013, **135**, 19083; c) A. Urtizberea and O. Roubeau, *Chem. Sci*., 2017, **8**, 2290.

17 T. Liu, H. Zheng, S. Kang, Y. Shiota, S. Hayami, M. Mito, O. Sato, K. Yoshizawa, S. Kanegawa and C. Duan. *Nature Commun*. 2013, **4**, 2826.

18 a) K. Takahashi, H.-B. Cui, Y. Okano, H. Kobayashi, H. Mori, H. Tajima, Y. Einaga and O. Sato, *J. Am. Chem. Soc*. 2008, **130**, 6688; b) H. Phan, S. M. Benjamin, E. Steven, J. S. Brooks and M. Shatruk, *Angew. Chem. Int. Ed.* 2015, **54**, 823.

19 a) I. Suleimanov, O. Kraieva, G. Molnár, L. Salmon and A. Bousseksou, *Chem. Commun*. 2015, **51**, 15098; b) I. Suleimanov, O. Kraieva, J. S. Costa, I.O. Fritsky, G. Molnár, L. Salmon and A. Bousseksou, *J. Mater. Chem*. *C* 2015, **3**, 5026.

20 C. Lochenie, K; Schötz, F. Panzer, H. Kurz, B. Maier, F. Puchtler, S. Agarwal, A. Köhler and B. Weber, *J. Am. Chem. Soc*., 2018, **140**, 700 and references therein.

21 P. Guionneau, M. Marchivie, G. Bravic, J.-F. Letard and D. Chasseau, *Top. Curr. Chem*. 2004, **234**, 97.

22 P. Guionneau, F. Le Gac, A. Kaiba, J. S. Costa, D. Chasseau and J.-F. Letard, *Chem. Commun*. 2007, 3723.

23 a) M. Nihei, H. Tahira, N. Takahashi, Y. Otake, Y. Yamamura, K. Saito and H. Oshio, *J. Am. Chem. Soc*. 2010, **132**, 3553; b) M. Yamasaki, T. Ishida and *J. Mater. Chem. C* 2015, **3**, 7784; c) T. Matsumoto, G. N. Newton, T. Shiga, S. Hayami, Y. Matsui, H. Okamoto, R. Kumai, Y. Murakami and H. Oshio, *Nature Commun*. 2014, **5**, 3865.

24 a) D. Rosario-Amorin, P. Dechambenoit, A. Bentaleb, M. Rouzières, C. Mathonière and R. Clérac, *J. Am. Chem. Soc*. 2018, **140**, 98; b) Milin, E. V. Patinec, S. Triki, E.-E. Bendeif, S. Pillet, M. Marchivie, G. Chastanet and K. Boukheddaden, *Inorg. Chem*. 2016, **55**, 11652; c) D. Zhang, E. Trzop, F. J. Valverde-Muñoz, L. Piñeiro-López, M. C. Muñoz, E. Collet and J. A. Real, *Cryst. Growth Des*. 2017, **17**, 2736.

25 a) S. Hayami, M. R. Karim and Y. H. Lee, *Eur. J. Inorg. Chem*. 2013, 683; b) A. B. Gaspar, M. Seredyuk and P. Gütlich, *Coord. Chem. Rev.* 2009, **253**, 2399; c) S. Hayami, Y. Shigeyoshi, M. Akita, K. Inoue, K. Kato, K. Osaka, M. Takata, R. Kawajiri, T. Mitani and Y. Maeda, *Angew. Chem., Int. Ed.,* 2005, **44**, 4899; d) S. Hayami, K. Kato, Y. Komatsu, A. Fuyuhiro and M. Ohba, *Dalton Trans.,* 2011, **40**, 2167; e) S. Hayami, K. Murata, D. Urakami, Y. Kojima, M. Akita and K. Inoue, *Chem. Commun.,* 2008, 6510; f) S. Hayami, D. Urakami, Y. Kojima, H. Yoshizaki, Y. Yamamoto, K. Kato, A. Fuyuhiro, S. Kawata and K. Inoue, *Inorg. Chem*. 2010, **49**, 1428; g) D. Rosario-Amorin, P. Dechambenoit, A. Bentaleb, M. Rouzières, C. Mathonière and R. Clérac, *J. Am. Chem. Soc.* 2018, **140**, 98; h) M. Seredyuk, A. B. Gaspar, V. Ksenofontov, Y. Galyametdinov, J. Kusz and P. Gütlich, *Adv. Funct. Mater.* 2008, **18**, 2089; i) G. Agusti, C. Bartual, V. Martinez, F. J. Munoz-Lara, A. B. Gaspar, M. C. Munoz and J. A. Real, *New J. Chem.,* 2009, **33**, 1262; j) S. Hayami, M. Nakaya, H. Ohmagari, A. S. Alao, M. Nakamura, R. Ohtani, R. Yamaguchi, T. Kuroda-Sowa and J. K. Clegg, *Dalton Trans.,* 2015, **44**, 9345-9348; k) K. Kuroiwa, T. Arie, S. Sakurai, S. Hayamic and T. J. Deming, *J. Mater. Chem. C,* 2015, **3**, 7779.

26 a) R. Bronisz, *Inorg. Chem.* 2007, **46**, 6733; b) A. Białońska, R. Bronisz, J. Kusz, M. Weselski and M. Zubko, *Eur. J. Inorg. Chem.* 2013, 875; c) A. Białońska, R. Bronisz, J. Kusz and M. Zubko, *Eur. J. Inorg. Chem.* 2013, 884; d) M. Książek, J. Kusz, A Białońska, R. Bronisz and M. Weselski, *Dalton Trans*., 2015, **44**, 18563; e) A. Białońska and R. Bronisz, *Inorg. Chem*. 2010, **49**, 4534; f) R. Bronisz, Z. Ciunik, K. Drabent and M. F. Rudolf, *Conf. Proc. ICAME-95* 1996, **50**, 15.

27 M. Weselski, M. Książek, P. Mess, J. Kusz and R. Bronisz, *Chem. Commun.,* 2019, **55**, 7033.

28 A. Białońska and R. Bronisz, *Inorg. Chem.* 2012, **51**, 12630.

29 a) J. Kusz, R. Bronisz, M. Zubko and G. Bednarek, *Chem. Eur. J.* 2011, **17**, 6807.

30 P. Chakraborty, C. Enachescu, A. Humair, L. Egger, T. Delgado, A. Tissot, L. Guénée, C.Besnard, R. Bronisz and A. Hauser, *Dalton Trans*., 2014, **43**, 17786.

31 M. Weselski, M. Książek, D. Rokosz, A. Dreczko, J. Kusz and R. Bronisz, *Chem. Commun*., 2018, **54**, 3895.

32 a) M. Książek, M. Weselski, M. Ilczyszyn, J. Kusz and R. Bronisz, *Chem. Eur. J*. 2019**, 25**, 2250; b) M. Książek, J. Kusz, A. Białońska, R. Bronisz and M. Weselski, *Dalton Trans*., 2015, **44**, 18563.

33 R. Bronisz, *Inorg. Chem.* 2005, **44**, 4463.

34 P. Chakraborty, R. Bronisz,; C. Besnard, L.Guénée, P. Pattison and A. Hauser, *J. Am. Chem. Soc*. 2012, **134**, 4049.

35 a) H. Hagiwara and S. A Okada, *Chem. Commun*. 2016, **52**, 815; b) H. Hagiwara, T. Tanaka and S. Hora, *Dalton Trans.* 2016, **45**, 17132; c) D. Schweinfurth, S. Demeshko, S. Hohloch, M. Steinmetz, J. G. Brandenburg, S. Dechert, F. Meyer, S. Grimme and B. Sarkar, *Inorg. Chem*. 2014, **53**, 8203; d) H. S. Scott, C. J. Gartshore, S.-X. Guo, B. Moubaraki, A. M. Bond, S. R. Batten and K. S. Murray, *Dalton Trans.* 2014, **43**, 15212; e) T. Romero-Morcillo, F. J. Valverde-Munoz, L. Pineiro-Lopez, M. C. Munoz, T. Romero and P. Molina, J. A. Real, *Dalton Trans*. 2015, **44**, 18911; f) H. Hagiwara, R. Minoura, S. Okada and Y. Sunatsuki, *Chem. Lett*. 2014, **43**, 950; g) H. Hagiwara, T. Masuda, T. Ohno, M. Suzuki, T. Udagawa and K. Murai, *Cryst. Growth Des*. 2017, **17**, 6006.

36 G. Aromí, L. A. Barriosa, O. Roubeau and P. Gamez, *Coord. Chem. Rev.,* 2001, **255**, 485.

37 F. J. Valverde-Munoz, M. Seredyuk, M. Meneses-Sanchez, M. C. Munoz, C. Bartual-Murguia and J. A. Real, *Chem. Sci*., 2019, **10**, 3807.

38 a) A. Tissot, P. Fertey, R. Guillot, V. Briois, M.-L. Boillot, *Eur. J. Inorg. Chem*. 2014, 101; b) S. Schönfeld, C. Lochenie, P. Thoma, B. Weber, *CrystEngComm*, 2015, **17**, 5389; V. Gómez, C. Sáenz de Pipaón, P. Maldonado-Illescas, J. C. Waerenborgh, E. Martin, J. Benet-Buchholz, J. Galán-Mascarós, *J. Am. Chem. Soc.* 2015, **137**, 11924; c) G. A. Craig, J. S. Costa, S. J. Teat, O. Roubeau, D. S. Yufit, J. A. K. Howard, G. Aromí, *Inorg. Chem*. 2013, **52**, 7203; d) V. Legrand, S. Pillet, C. Carbonera, M. Souhassou, J.-F. Létard, P. Guionneau, C. Lecomte, *Eur. J. Inorg. Chem.* 2007, 5693; e) G. A. Craig, J. S. Costa, O. Roubeau, S. J. Teat, H. J. Shepherd, M. Lopes, G. Molnár, A. Bousseksou, G. Aromí, *Dalton Trans.,* 2014, **43**, 729; f) S. Heider, H. Petzold, G. Chastanet, S. Schlamp, T. Rüffer, B. Weber, J.-F. Létard, *Dalton Trans.,* 2013, **42**, 8575; g) G. A. Craig, J. S. Costa, O. Roubeau, S. J. Teat, G. Aromi, *Chem. Eur. J.* 2011, **17**, 3120; h) A. Moneo-Corcuera, D. Nieto-Castro, C. Sáenz de Pipaón, V. Gómez, P. Maldonado-Illescasa, J. R. Galan-Mascaros, *Dalton Trans.,* 2018, **47**, 11895; i) T. Boonprab, S. J. Lee, S. G. Telfer, K. S. Murray, W. Phonsri, G. Chastanet, E. Collet, E. Trzop,; G. N. L.

View Article Online
DOI: 10.1039/D0DT01696A

View Article Online
DOI: 10.1039/D0DT01696A

Jameson, P. Harding, D. J. Harding, *Angew. Chem.* 2019, **131**, 11937.

39 a) C. Knoll, D. Müller, M. Seifried, G. Giester, J. M. Welch, W. Artner, K. Hradil, M. Reissner, P. Weinberger, *Dalton Trans.,* 2018, **47**, 5553; B) M. Quesada, F. Prins, E. Bill, H. Kooijman, P. Gamez, O. Roubeau, A. L. Spek, J. G. Haasnoot, J. Reedijk, *Chem. Eur. J.*, 2008, **14**, 8486.

40 R. J. Archer, H. S. Scott, M. I. J. Polson, C. Mathoniere, M. Rouzieres, R. Clerac, P. E. Kruger, *Chem. Asian J.* **2019**, *14*, 2225.

41 D. Bradley, G. Williams and M. Lawton, *J. Org. Chem*., 2010, **75**, 8351.

42 CrysAlis^{Pro}. Version 1.171.35.21b, Oxford Diffraction Ltd., 2012.

43 CrysAlis^{Pro}. Version 1.171.38.41q, Rigaku Oxford Diffraction, 2015.

44 G. M. Sheldrick, *Acta Cryst.* 2015, **C71**, 3.

45 M. Begtrup, P. Larsen, P. *Acta Chem. Scand*. 1990, **44**, 1050.

View Article Online
DOI: 10.1039/D0DT01696A

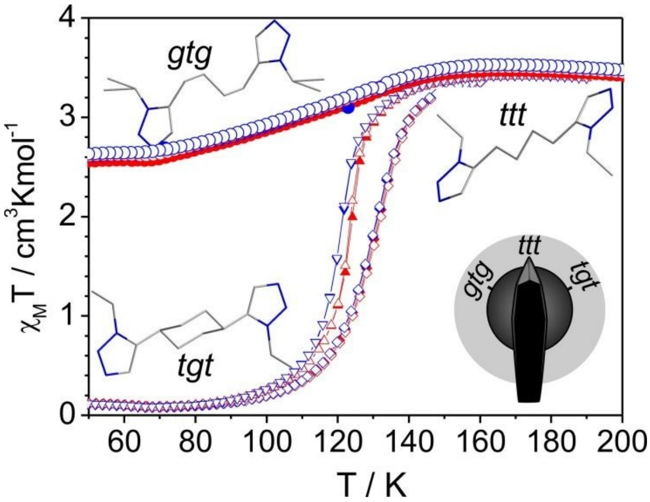

Structural phase transition in [Fe(**bbtre**)$_3$](ClO$_4$)$_2$·2CH$_3$CN (**bbtre**=1,4-di(1-ethyl-1,2,3-triazol-5-yl)butane) playes a role of switch allowing to carry out spin crossover in two ways.